

Supporting information

Zeolite-templated nanoporous carbon for high-performance supercapacitors

Hao Lu,^a Kyoungsoo Kim,^b Yonghyun Kwon,^{b,c} Xiaoming Sun,^a Ryong Ryoo*^{a,b,c} and X. S. Zhao*^a

^aSchool of Chemical Engineering, The University of Queensland, St Lucia, Brisbane, QLD 4072, Australia. E-mail: george.zhao@uq.edu.au (X. S. Zhao)

^bCenter for Nanomaterials and Chemical Reactions, Institute for Basic Science (IBS), Daejeon 34141, Republic of Korea.

^cDepartment of Chemistry, KAIST, Daejeon 34141, Republic of Korea. E-mail: rryoo@kaist.ac.kr (R. Ryoo)

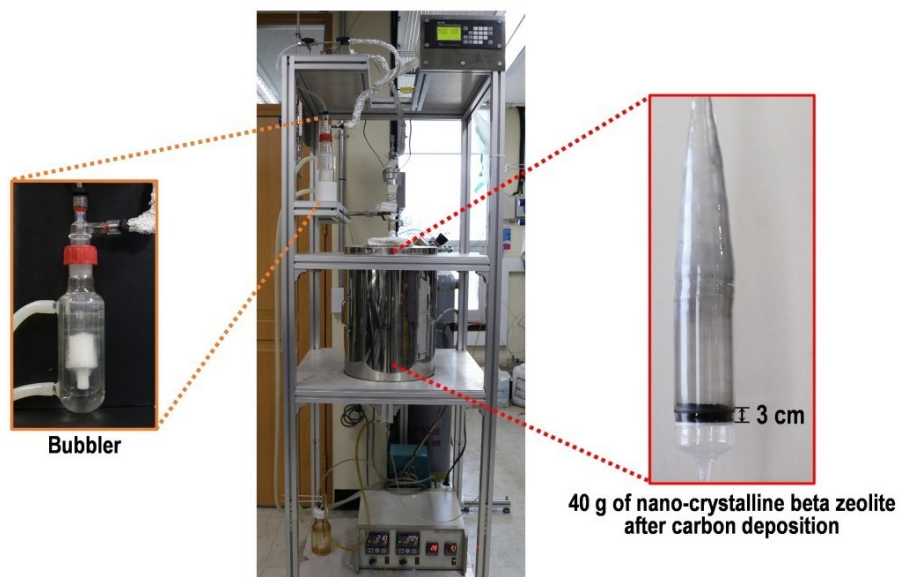


Fig.S1. Photograph of the carbon deposition rig for carbon synthesis in a large-scale. N_2 /ethylene mixture was bubbled through water before reaching a zeolite bed (left inset). A 3 cm-thick bed of zeolite filled in the plug-flow reactor equipped with a fritted disk was used in the synthesis (right inset).

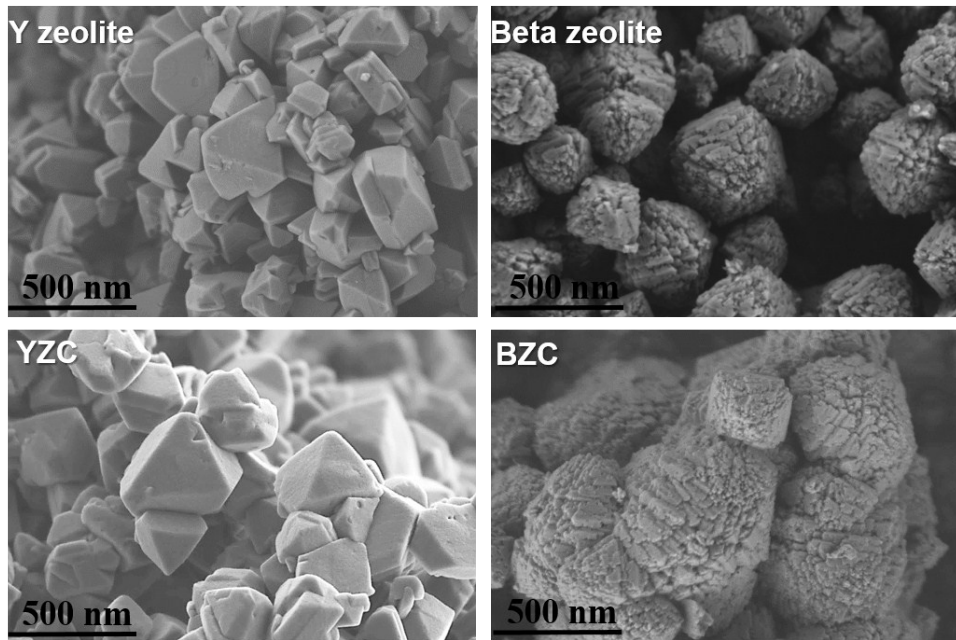


Fig. S2. SEM images of YZC and BZC, and their separate template.

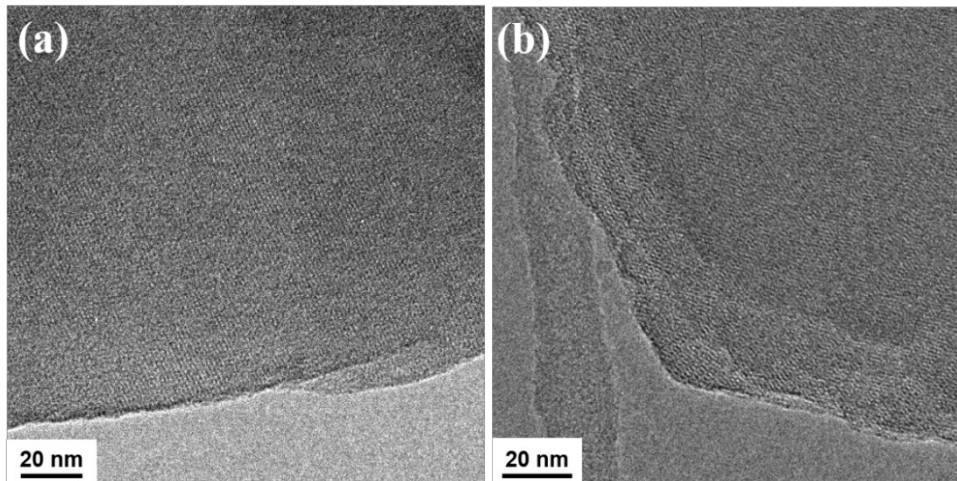


Fig. S3. TEM images of YZC and BZC.

Fig. 2a schematically shows the carbon deposition process using calcium-containing zeolites as templates. Firstly, the ion exchange for Na^+ containing template with Ca^{2+} was conducted. Then the Ca-containing template was heated at $600\text{ }^\circ\text{C}$ for 1 h under ethylene flow, followed by heat treatment at $850\text{ }^\circ\text{C}$ for 2 h under N_2 atmosphere. The Ca^{2+} can promote the ethylene carbonization, which lowers the carbonization temperature, thus preventing the non-selective carbon deposition at the external surfaces.^{1, 2} Finally, the sample was washed with HF/HCl solution, which washes away the zeolite template and simultaneously

adds certain content of oxygen-containing surface functional groups, contributing to pseudocapacitance. The SEM images (Fig. 2b-c, Fig. S2) show that the carbon products were all good replica of their separate template. The TEM images in Fig. 2d and Fig. S3 show ordered porous structure of the carbons. Especially the TEM image in Fig. 2d and the HRTEM image in Fig. 2e show ordered mesoporous/microporous structure of NBZC, revealing the selective deposition of carbon inside the template, which was further confirmed by the XRD results in Fig. S4.^{1,3,4}

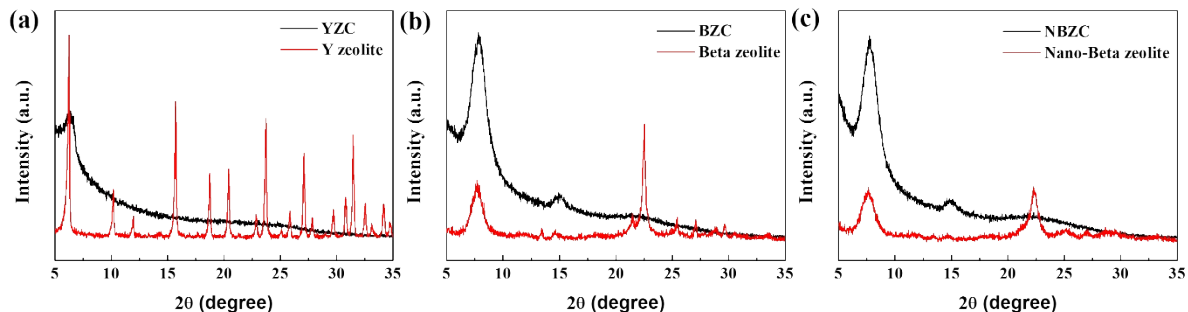


Fig. S4. XRD patterns of YZC, BZC, and NBZC and their separate template. The carbons show a well-resolved peak at $2\theta \approx 7^\circ$, which corresponds to the (100) or (101) diffraction of the templates, indicating the ordered micropores in the carbons.^{1,3,4}

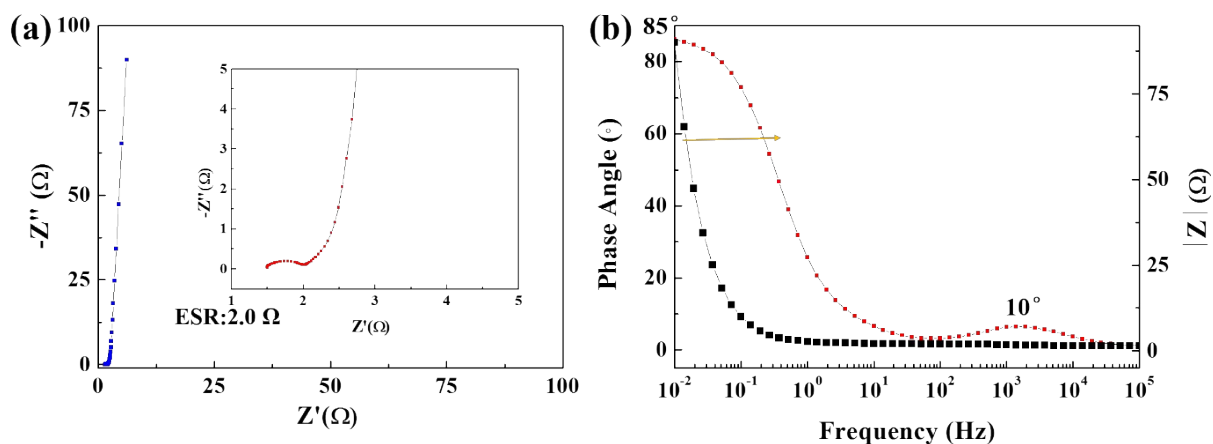


Fig. S5. (a) Nyquist plot, (b) Bode plots of NBZC in a three-electrode system with 1 M H_2SO_4 as aqueous electrolyte.

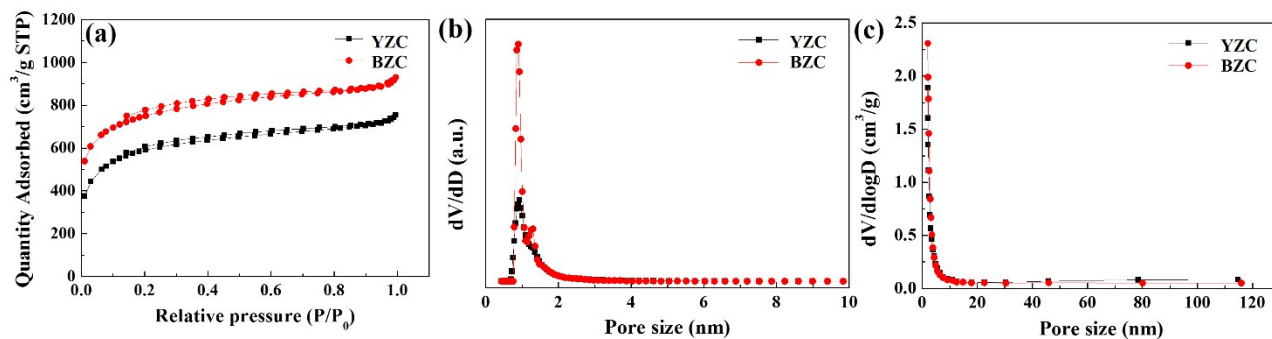


Fig. S6. N₂ adsorption/desorption isotherms (a) and pore size distributions calculated using the DFT model (b) and BJH model (c) of YZC and BZC.

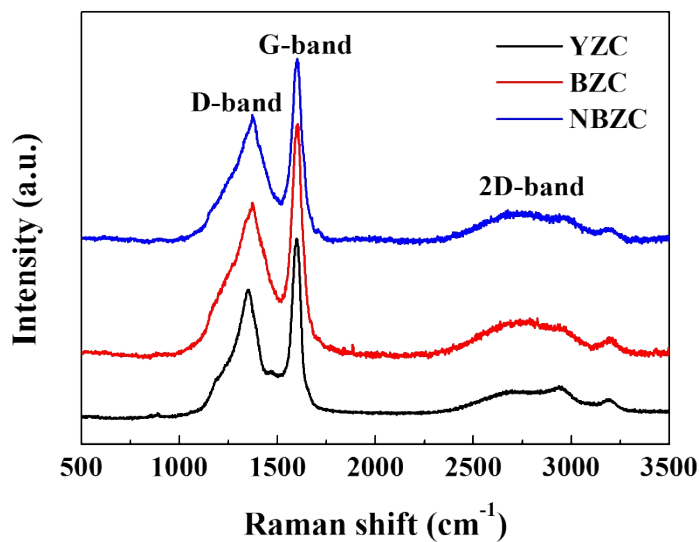


Fig. S7. Raman spectra of YZC, BZC, and NBZC.

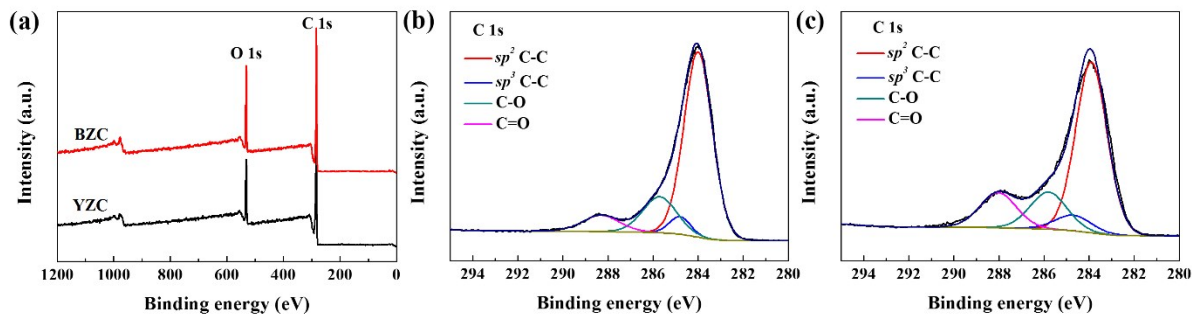


Fig. S8. XPS survey spectra of YZC and BZC (a), C 1s envelope of YZC (b) and BZC (c).

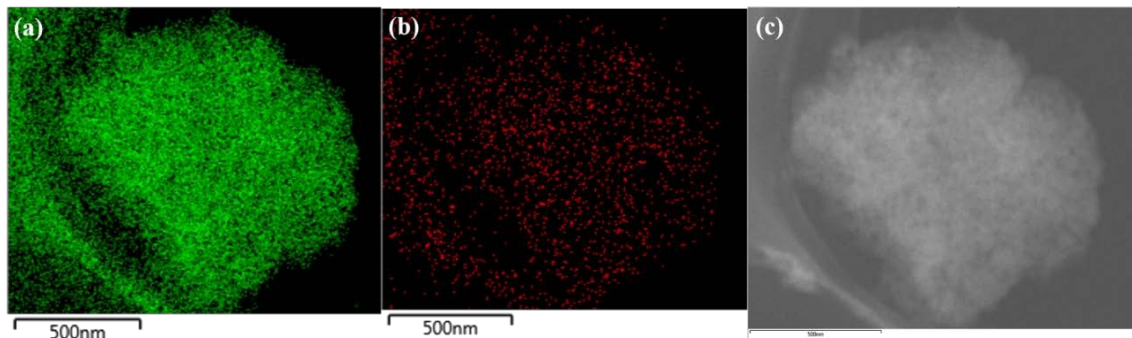


Fig. S9. STEM-EDS mapping of C (a), O (b) and HAADF-STEM image (c) of NBZC.

The chemical composition of NBZC was characterised using the scanning transmission electron microscopy - energy dispersive spectrometer (STEM - EDS) and XPS techniques. The STEM - EDS images, Figs. S9a-b, and the STEM image conducted in a high-angle annular dark field mode (HAADF - STEM), Fig. S9c, show that oxygen uniformly presents in the sample. The XPS survey spectrum of NBZC is shown in Fig. 4a. The two distinct peaks at 284.4 eV and 532 eV correspond to binding energies of C 1s and O 1s electrons, respectively. The quantitative analysis of the spectrum showed that it contains 90.8 at% C and 9.2 at% O. The presence of oxygen was due to partial oxidation of the carbon framework during the zeolite template removal process using HF/HCl solution. This process involves heat generation and the heat increases with the amount of washed samples. Therefore, the oxygen content of the carbon prepared in a large scale is slightly higher than that of the one prepared in a small scale. Fig. 4b shows the deconvolution of C 1s peak. Four peaks corresponding to sp^2 C-C (284.4 eV), sp^3 C-C (285.2 eV), C-O (286.1 eV) and C=O (288.4 eV) can be seen.^{1,5} The O 1s peaks at 531.3 and 532.8 eV correspond to C=O and C-O respectively.⁶

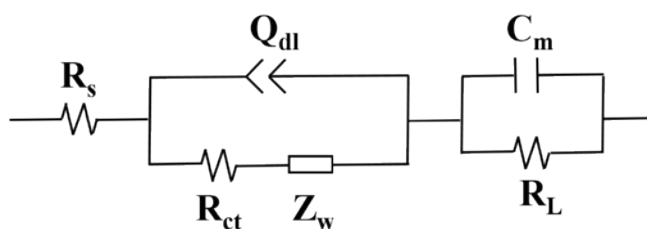


Fig. S10. Equivalent circuit used for the simulation of EIS data.

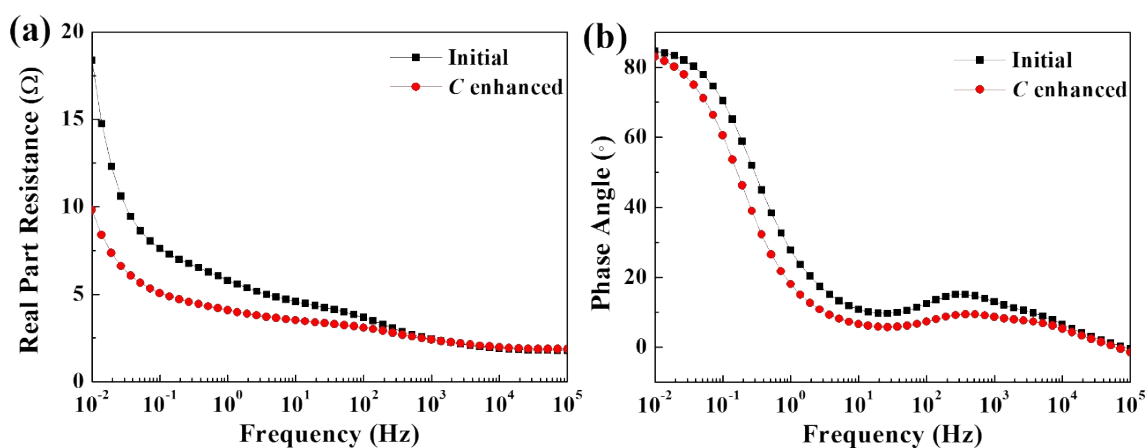


Fig. S11. Real part resistance vs frequency (a) and Bode phase angle plots (b) of the symmetric capacitor with 1 M H_2SO_4 as the electrolyte of NBZC.

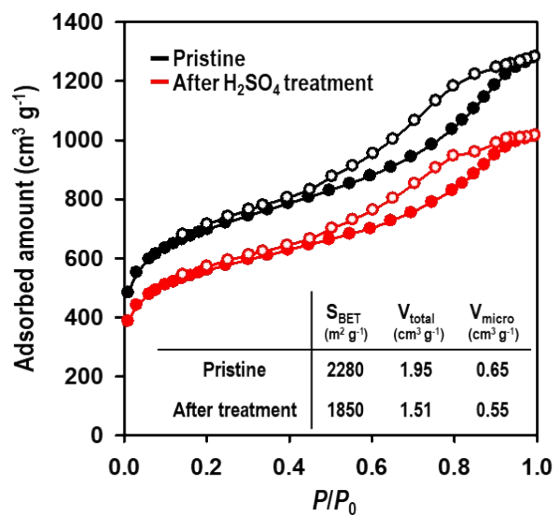


Figure S12. N_2 adsorption-desorption isotherms and textural properties (inset) of the sample NBZC before and after 1 M H_2SO_4 treatment for 1 d at 25 °C.

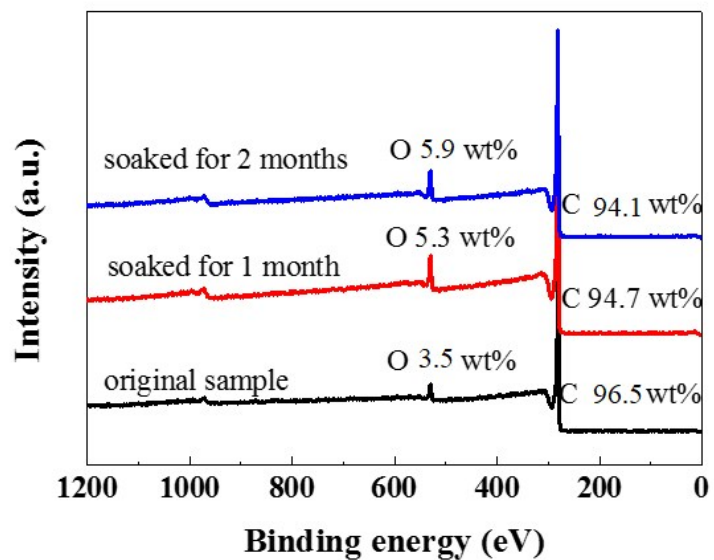


Figure S13. XPS survey spectra of original sample NBZC as well as that of soaked after 1 month and 2 months.

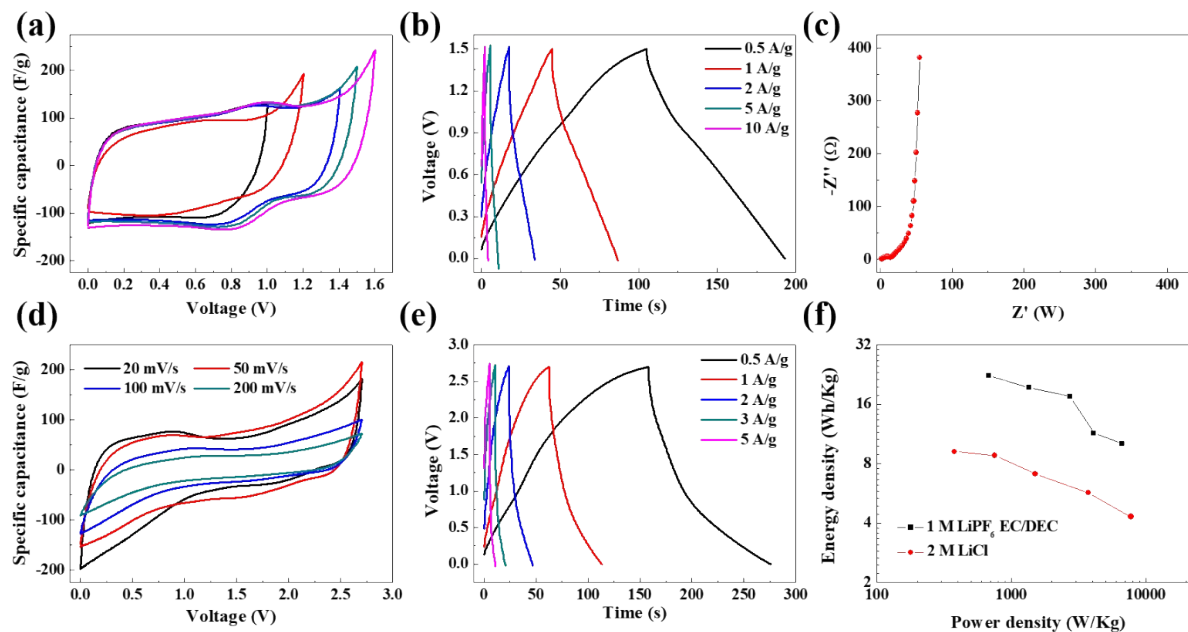


Fig. S14. Electrocapacitive performance of electrode NBZC in a symmetric cell with 2 M LiCl (a, b, c) or 1 M LiPF₆ EC/DEC (d, e, f) as electrolyte.

The real part specific capacitance (C'):

$$C'(\omega) = \frac{-Z''(\omega)}{\omega |Z(\omega)|^2} \quad (1)$$

The imagine part specific capacitance (C'')

$$C''(\omega) = \frac{Z'(\omega)}{\omega |Z(\omega)|^2} \quad (2)$$

Table S1. Specific capacitance values of NBZC at different current densities in a three-electrode system with 1 M H₂SO₄ as aqueous electrolyte.

Current density (A/g)	0.2	0.5	1	2	5	10	15	20
C_s (F/g)	307	268	250	235	215	199	189	177

Table S2. Comparison of the preparation and properties of porous carbon materials and their use in SCs

Carbon precursor	Carbon-based electrodes	Pore structure	Preparation method	SSA (m ² /g)	Specific capacitance	Cycle stability	Ref.
Carbon nanofibers	Nitrogen-doped porous carbon nanofibers	Micro/meso/macroporous	Carbonization	562	202 F/g at 1 A/g, three-electrode, 6M KOH	97 % retention after 3000 cycles at 1 A/g	7
Lignin	Porous lignin-derived carbon	3D hierarchically porous	KOH activation	907	185 F/g at 0.05 A/g, two-electrode, 1M H ₂ SO ₄	97.3 % retention after 5000 cycles at 1 A/g	8
Polypyrrole microsheets	Nitrogen-doped porous carbon	3D hierarchically micro/meso/macroporous	KOH activation	2870	318 F/g at 0.5 A/g, three-electrode, 6M KOH	95.8 % retention after 10000 cycles at 5 A/g	9
Eggshell membranes	Porous carbon film	3D macroporous	Air activation	221	284 F/g at 0.2 A/g, three-electrode, 1M H ₂ SO ₄	97 % retention after 10000 cycles at 4 A/g	10
Pig bone	Porous carbon	Hierarchically micro/meso/macroporous	KOH activation	2157	185 F/g at 0.05 A/g, two-electrode, 7M KOH	-	11
Pitch	pillared-porous carbon nanosheet	3D mesoporous	MgO-template	883	289 F/g at 2 mV/s, three-electrode, 6M KOH	94 % retention after 10000 cycles at 200 mV/s	12
GO	RGO hydrogel film	Hierarchically meso/macroporous	Blade-cast and freeze drying	1316	71 mF/cm ² at 1 mA/cm ² , two-electrode, 1M H ₂ SO ₄	98 % retention after 5000 cycles at 10 mA/cm ²	13
Flaked graphite	RGO film	3D porous	CaCO ₃ -template	-	~125 F/g at 0.5 A/g, two-electrode, 1M H ₂ SO ₄	90 % retention after 5000 cycles at 5 A/g	14
Glucose	Porous carbon hollow spheres	Micropore shell with meso/micropore cores	Colloidal silica hard template	658	269 F/g at 0.5 A/g, three-electrode, 6M KOH	92 % retention after 1000 cycles at 5 A/g	15
Gelatin	Nitrogen-doped porous carbon	Microporous/mesoporous	Dual-template	1518	110 F/g at 2 A/g, two-electrode cell, 1M EMIMBF ₄ /AN	98.2% retention after 10000 cycles at 20 A/g	16
Phenolic resol	Porous carbon spheres	3D Mesoporous	Dual-template	1320	208 F/g at 0.5 A/g, three-electrode, 2M H ₂ SO ₄	~100 % retention after 1000 cycles at 1.59 A/g	17
PAN	Nitrogen-doped carbon nanofibers	Hierarchically micro/mesoporous	Dual-template	699	170 F/g at 1 A/g, two-electrode, 6M KOH	94 % retention after 8000 cycles at 1 A/g	18
Coal tar pitch	Hierarchical porous carbon	Hierarchically micro/mesoporous	Fe ₂ O ₃ -template and KOH activation	1330	194 F/g at 0.1 A/g, two-electrode, 6M KOH	93.2 % retention after 1000 cycles at 0.1 A/g	19
Gelatin	Porous carbon nanosheets	2D porous carbon nanosheet	Montmorillonite-template and KOH activation	2270	228 F/g at 1 A/g, two-electrode, 6M KOH	-	20
MOF-5	Porous carbon	Microporous/mesoporous	MOF-template and KOH activation	2222	271 F/g at 2 mV/s, three-electrode, 6M KOH	-	21
Ethylene	Porous carbon	3D hierarchically micro/mesoporous	calcium-catalysed zeolite-template	2280	307 F/g at 0.2 A/g, three-electrode, 1M H ₂ SO ₄ 413 mF/cm ² at 0.25 mA/cm ² , two-electrode, PVA/ H ₂ SO ₄ (active material area of 1 cm ² , mass loading of 2 mg/cm ²)	153 % retention two-month-shelfing time after 17000 cycles at 1 A/g	This work

Table S3. Areal specific capacitance values of NBZC at different current densities in an all-solid-state capacitor with PVA / H₂SO₄ gel as the electrolyte.

Current density (mA/cm ²)	0.25	0.5	1	2	5	10	15	20
C _a (mF/cm ²)	413	400	380	358	314	246	197	160

Reference

1. K. Kim, T. Lee, Y. Kwon, Y. Seo, J. Song, J. K. Park, H. Lee, J. Y. Park, H. Ihee and S. J. Cho, *Nature*, 2016, **535**, 131-147.
2. Z. Yang, Y. Xia and R. Mokaya, *J. Am. Chem. Soc.*, 2007, **129**, 1673-1679.
3. K. Kim, M. Choi and R. Ryoo, *Carbon*, 2013, **60**, 175-185.
4. Y. Xia, Z. Yang and R. Mokaya, *Nanoscale*, 2010, **2**, 639-659.
5. L. Sun, C. Tian, M. Li, X. Meng, L. Wang, R. Wang, J. Yin and H. Fu, *J. Mater. Chem. A*, 2013, **1**, 6462-6470.
6. S. Song, F. Ma, G. Wu, D. Ma, W. Geng and J. Wan, *J. Mater. Chem. A*, 2015, **3**, 18154-18162.
7. L.-F. Chen, X.-D. Zhang, H.-W. Liang, M. Kong, Q.-F. Guan, P. Chen, Z. Y. Wu and S. H. Yu, *ACS nano*, 2012, **6**, 7092-7102.
8. W. Zhang, H. Lin, Z. Lin, J. Yin, H. Lu, D. Liu and M. Zhao, *ChemSusChem*, 2015, **8**, 2114-2122.
9. L. Qie, W. Chen, H. Xu, X. Xiong, Y. Jiang, F. Zou, X. Hu, Y. Xin, Z. Zhang and Y. Huang, *Energy Environ. Sci.*, 2013, **6**, 2497-2504.
10. Z. Li, L. Zhang, B. S. Amirkhiz, X. Tan, Z. Xu, H. Wang, B. C. Olsen, C. Holt and D. Mitlin, *Adv. Energy Mater.*, 2012, **2**, 431-437.
11. W. Huang, H. Zhang, Y. Huang, W. Wang and S. Wei, *Carbon*, 2011, **49**, 838-843.
12. Z. Fan, Y. Liu, J. Yan, G. Ning, Q. Wang, T. Wei, L. Zhi and F. Wei, *Adv. Energy Mater.*, 2012, **2**, 419-424.
13. Z. Xiong, C. Liao, W. Han and X. Wang, *Adv. Mater.*, 2015, **27**, 4469-4475.
14. Y. Meng, K. Wang, Y. Zhang and Z. Wei, *Adv. Mater.*, 2013, **25**, 6985-6990.
15. Y. Han, X. Dong, C. Zhang and S. Liu, *J. Power Sources*, 2012, **211**, 92-96.
16. X. Y. Chen, C. Chen, Z. J. Zhang and D. H. Xie, *J. Mater. Chem. A*, 2013, **1**, 10903-10911.
17. Q. Li, R. Jiang, Y. Dou, Z. Wu, T. Huang, D. Feng, J. Yang, A. Yu and D. Zhao, *Carbon*, 2011, **49**, 1248-1257.
18. Q. Wang, Q. Cao, X. Wang, B. Jing, H. Kuang and L. Zhou, *J. Solid State. Electrochem.*, 2013, **17**, 2731-2739.
19. X. He, N. Zhao, J. Qiu, N. Xiao, M. Yu, C. Yu, X. Zhang and M. Zheng, *J. Mater. Chem. A*, 2013, **1**, 9440-9448.

20. X. Fan, C. Yu, J. Yang, Z. Ling, C. Hu, M. Zhang and J. Qiu, *Adv. Energy Mater.*, 2015, **5**, 14011761.
21. J. Hu, H. Wang, Q. Gao and H. Guo, *Carbon*, 2010, **48**, 3599-3606.